

Physics-informed Learning for Identification and State Reconstruction of Traffic Density

Matthieu Barreau¹, Miguel Aguiar¹, John Liu¹ and Karl Henrik Johansson¹

Abstract—This paper deals with traffic density reconstruction using measurements from Probe Vehicles (PVs). The main difficulty arises when considering a low penetration rate, meaning that the number of PVs is small compared to the total number of vehicles on the road. Moreover, the formulation assumes noisy measurements and a partially unknown first-order model. All these considerations make the use of machine learning to reconstruct the state the only applicable solution. We first investigate how the identification and reconstruction processes can be merged and how a sparse dataset can still enable a good identification. Secondly, we propose a pre-training procedure that helps the hyperparameter tuning, preventing the gradient descent algorithm from getting stuck at saddle points. Examples using numerical simulations and the SUMO traffic simulator show that the reconstructions are close to the real density in all cases.

I. INTRODUCTION

Traffic state control has recently attracted a lot of attention [1]. The possibility, in a near future, of using automated vehicles within the flow of vehicles opened many new control and observation perspectives.

There are two classical methods for traffic state reconstruction. The most used one relies on a model, and is therefore labeled model-based. The survey [2] gives a good overview of many different modern techniques. The use of probe vehicles in this context is however quite recent and the reader can refer to [3], [4]. Nevertheless, for more complex models or robustness issues, it is today almost impossible to use macroscopic models. This is in part due to the fact that it is very difficult, mathematically speaking, to derive convergence properties for infinite-dimensional nonlinear systems.

Another approach that is widely used today is called data-based or data-driven [5]. Such a methodology uses measurement data to derive system properties or predict the near future. This has been used in traffic state reconstruction in [6] for instance. The approach is quite powerful since it does not require many assumptions and the generality is quite high. However, there are not many practical applications since it requires many in-domain measurements. This is conceivable when using probe vehicles, but it assumes a large penetration rate, meaning that most of the vehicles are capable of probing.

To get the advantages of both methods while avoiding the aforementioned difficulties, it is of interest to develop a

data-model driven methodology. This has recently been done in [7], [8] using the notion of physics-informed learning. This data-based technique enforces a physical model on the measurements such that the generalization error is kept small even when the measurements are few and sparse.

This approach has had a very large impact on the scientific community. The problem of traffic state reconstruction has recently been investigated using this methodology in [9] and further in [10], [11]. The use of probe vehicles in particular is studied in [12]. The application to traffic flow reconstruction with data coming from external simulators is considered in [13].

The objective of this paper requires some definitions before we are able to state it precisely. However, informally speaking, the aim is to derive an algorithm capable of estimating the density of cars from sporadic measurements taken by probing cars on the road. The main contribution is the development of a machine learning framework for joint identification and state estimation of traffic flow from sparse measurements taken by probe vehicles. In comparison with our previous papers [12], [13], which focused on state estimation, here we consider in addition the problem of identifying the velocity function. Such a difference implies an explosion of the number of variables and physical costs. The second contribution lies in the enhanced training procedure so that it can deal with many constraints simultaneously.

The paper is organized as follows. In Section 2, we will introduce two traffic models. Section 3 is dedicated to the mathematical formulation of the objective in terms of an optimization problem and introduces a relaxed version of the problem. Section 4 proposes a learning solution focusing on the training procedure. Section 5 discusses the results obtained in different settings. Finally, Section 6 concludes with some perspectives on future research directions.

Notation: We define $L^1_{\text{loc}}(\mathcal{S}_1, \mathcal{S}_2)$, $L^\infty(\mathcal{S}_1, \mathcal{S}_2)$ and $C^k(\mathcal{S}_1, \mathcal{S}_2)$ as the spaces of locally integrable functions, bounded functions and continuous functions of class k from \mathcal{S}_1 to \mathcal{S}_2 , respectively. Let $f \in C^1$ be a function of time and space, we denote by \dot{f} or f_t its time derivative and by f' or f_x its space derivative.

II. COUPLED MACRO-MICRO MODEL OF TRAFFIC FLOW

There are two main kinds of traffic models in the literature, namely macroscopic and microscopic models [1]. These two model types are briefly discussed in this first section to explain the benefit of using a coupled micro-macro model of traffic flow.

¹ Division of Decision and Control Systems, KTH Royal Institute of Technology, Stockholm, Sweden (e-mail: {barreau, aguiar, johnliu, kallej}@kth.se).

This research is partially funded by the KAUST Office of Sponsored Research under Award No. OSR-2019-CRG8-4033, the Swedish Foundation for Strategic Research and Knut and Alice Wallenberg Foundation.

A. Microscopic model

Assume here that there are $N > 1$ vehicles located at position $y_i \in \mathbb{R}$ for $i \in \{1, \dots, N\}$. First order microscopic models assume that the following dynamic equation holds:

$$\begin{cases} \dot{y}_i(t) = V(y_{i+1}(t) - y_i(t)) & \text{if } i \in \{1, \dots, N-1\}, \\ \dot{y}_N(t) = V_{\text{leader}}(t), \\ y_1(0) < \dots < y_N(0). \end{cases}$$

This is a classical follow-the-leader dynamical system with $V_{\text{leader}} \geq 0$. Usually, the velocity function V is a function of the intra-vehicular space and it is a decreasing, bounded and positive function.

Such models perform badly in practice since they are too simple. Second-order models have been introduced to improve the correlation with real-life measurements [1]. The SUMO traffic simulator [14] implements an elaborated version of second order follow-the-leader dynamics. Another drawback is that the system dimension becomes very large when dealing with many vehicles. To this extent, one can introduce an infinite-dimensional model, referred to as a macroscopic model.

B. Macroscopic model

a) Notion of density: From the previous model, one can define the *normalized density of vehicles* ρ such that:

$$N_{\text{veh}}(x_1, x_2, t) = \rho_{\max} \int_{x_1}^{x_2} \rho(t, x) dx,$$

where $N_{\text{veh}}(x_1, x_2, t)$ is the number of vehicles at a given time t on the segment of road $[x_1, x_2]$. As explained in [12], [15], the normalized density is then a solution to the hyperbolic equation:

$$\rho_t(t, x) + f(\rho(t, x))_x = 0 \quad (1)$$

with $\rho : \mathbb{R}_{\geq 0} \times \mathbb{R} \rightarrow [0, 1]$, an initial condition $\rho(0, \cdot) = \rho_0$, and a smooth and concave function $f : \mathbb{R} \rightarrow \mathbb{R}_{\geq 0}$.

If $\rho(t, x)$ is thought of as the normalized density of some substance at time t and location x , we see that (1) is the conservation of mass equation when f is the flux, i.e. $f(\rho)$ is the rate at which the substance is passing through a point with density ρ . Then we can also define the substance velocity $v : [0, 1] \rightarrow \mathbb{R}_{\geq 0}$ through the relation

$$\rho v(\rho) = f(\rho). \quad (2)$$

In traffic applications, the ‘substance’ in question refers to the vehicles on a road, as from a macroscopic point of view one assumes that the flow of vehicles can be approximated by the flow of a continuous substance. Then $f(\rho)$ gives the number of vehicles flowing through some point of space per unit time, and $v(\rho)$ is the mean vehicle velocity.

One can rewrite (1) as

$$\rho_t(t, x) + F(\rho(t, x))\rho_x(t, x) = 0$$

where $F = f'$. Then F is the speed of the characteristic curves, that is, if $x : \mathbb{R}_{\geq 0} \rightarrow \mathbb{R}$ is a solution of $\dot{x}(t) = F(\rho(t, x(t)))$ then $t \mapsto (t, x(t))$ is a curve of constant density in the (t, x) plane.

b) Existence of a solution: It is well known that there may be no smooth solution of (1), even for smooth initial data. Hence we consider solutions in a weak sense, and one then has the following existence and stability result [12]:

Theorem 1: If $\rho_0 \in L^\infty(\mathbb{R}, [0, 1])$ and $f \in C^2([0, 1], \mathbb{R}_{\geq 0})$, then there exist weak solutions ρ of (1) with regularity $\rho \in C^0(\mathbb{R}_{\geq 0}, L^1_{\text{loc}}(\mathbb{R}, [0, 1]))$.

Uniqueness is ensured by restricting the set of weak solutions to those satisfying the Lax-E condition [16, Chap. 14]. An alternative way to obtain a unique solution is to consider smooth solutions to the related equation

$$\bar{\rho}_t(t, x) + f(\bar{\rho}(t, x))_x = \gamma^2 \bar{\rho}_{xx}(t, x) \quad (3)$$

for small γ . If ρ_γ is the solution of (3), then the limit $\rho := \lim_{\gamma \downarrow 0} \rho_\gamma$ exists in a weak sense in L^1_{loc} [16, p. 157] and is the entropic solution of (1).

c) Examples of flux functions: The two most well-known flux functions used in traffic applications are perhaps the Greenshields [17] and the Newell-Daganzo [18], [19] flux functions. The Greenshields flux function f_G is given by

$$f_G(\rho) = \rho v_G(\rho), \quad v_G(\rho) = V_f(1 - \rho). \quad (4)$$

At zero traffic density the vehicles move at the free flow velocity $V_f > 0$, and the velocity v_G decreases linearly with density, going to zero as the road becomes more congested.

The Newell-Daganzo flux function is given by

$$f_{\text{ND}}(\rho) = \min \{V_f \rho, W(1 - \rho)\}. \quad (5)$$

The velocity function in this case is then

$$v_{\text{ND}}(\rho) = \begin{cases} V_f, & \rho < \sigma, \\ W \frac{1-\rho}{\sigma}, & \rho \geq \sigma, \end{cases}$$

where $\sigma \in [0, 1]$ is such that $V_f \sigma = W(1 - \sigma)$. Hence vehicles move at a constant average velocity up to a critical density σ where the road becomes congested, and the velocity goes to zero as ρ approaches one.

Remark 1: The flux function in this case is not differentiable everywhere. One can then consider a convolution to make f_{ND} smoother such that Theorem 1 applies. \square

C. Relation between the models

The two models introduced so far are mathematically related. The Greenshields model is a limit case of the first order follow-the-leader dynamics [20] and the integral of the normalized density is proportional to the number of vehicles. Consequently, ρ is directly related to the intra-vehicular space and one can use the velocity function v of the macroscopic scheme as the vehicle velocity V [13]. That leads to the following cascaded system:

$$\begin{cases} \dot{y}_i(t) = v(\rho(t, y_i(t)^+)) & \text{for } i \in \{1, \dots, N\}, \\ \rho_t(t, x) + f(\rho(t, x))_x = \gamma \rho_{xx}(t, x), & (t, x) \in \mathbb{R}_{\geq 0} \times \mathbb{R}, \end{cases} \quad (6)$$

with appropriate initial conditions. In [12] the authors give conditions for (6) to be mathematically well-posed.

Definition 1: For the two models to be self-consistent, one must ensure the following :

- 1) f must be positive, concave and C^2 ;
- 2) v must be positive and decreasing;
- 3) v must be always larger than or equal to F .

Remark 2: The last item is related to observability [3] and is discussed in Remark 5. \square

The following proposition gives a simple sufficient condition for consistency of the models.

Proposition 1: If f is concave and $v \in C^2([0, 1], \mathbb{R}_{\geq 0})$, then equation (6) is a consistent model for describing micro- and macroscopic behaviors of traffic flow.

Proof: From the assumptions and using (2), we get that $f(0) = 0$ and f is positive. By concavity of f , the Chordal Slope Lemma implies that v is decreasing. Since $F(\rho) = f'(\rho) = v(\rho) + \rho v'(\rho)$, we get that $F - v$ has the same sign as v' which is negative. Consequently, Definition 1 indeed holds and the model is consistent. \blacksquare

For the sequel, the best is to express f and F as a function of v . Using (2), we get:

$$\begin{cases} F(\rho) = f'(\rho) = v(\rho) + \rho v'(\rho), \\ f''(\rho) = 2v'(\rho) + \rho v''(\rho). \end{cases} \quad (7)$$

Combining (6), (7), Proposition 1 and Definition 1 leads to the following for $i \in \{1, \dots, N\}$:

$$\begin{cases} \mathcal{N}_y[y_i] = \dot{y}_i - v(\rho(\cdot, y_i^+)) = 0, \\ \mathcal{N}_\rho[\rho, v] = \rho_t + (v(\rho) + \rho v'(\rho)) \rho_x - \gamma^2 \rho_{xx} = 0, \\ \mathcal{N}_v[v] = 2v' + \rho v'' \leq 0, \\ v \geq 0 \text{ and } C^2. \end{cases} \quad (8)$$

Remark 3: Note that with the Greenshields or the regularized Newell-Daganzo speed function, the two last statements of (8) are indeed verified, resulting in a consistent model. \square

D. Measurements

In this paper probe vehicles are used as mobile sensors within the flow of vehicles. These vehicles are special in that they can estimate the three following values in real-time:

- 1) Their positions $y_i(t)$;
- 2) The local density at their locations: $\rho_i(t) = \rho(t, y_i(t))$;
- 3) And their instantaneous speed $v_i(t) = \dot{y}_i(t)$;

Requiring measurements 1 and 3 is reasonable since these only require the use of GPS or inertial data. The density measurements are more delicate. In a single-lane environment, one can measure the inter-vehicular distances and deduce an approximation of the local density. In a multi-lane context, a camera or radar sensors might be needed [21].

Remark 4: Compared to the authors' previous work [13], we need to measure the instantaneous speed since we do not make any assumptions on the velocity-density relation. \square

One can then study the state-reconstruction problem based on equation (8).

III. PROBLEM STATEMENT

The general definition of partial-state reconstruction is proposed in [12]. Here, we adapt this definition to get a density reconstruction.

Definition 2: Let $\Omega = [0, T]$, $T > 0$. A **density reconstruction** $\hat{\rho}$ in $\mathcal{H}_c \subset H^1(\Omega, H^2(\mathbb{R}, [0, 1]))$ is defined as

$$\hat{\rho} \in \underset{\bar{\rho} \in \mathcal{H}_c}{\text{Argmin}} \sum_{i=1}^N \int_0^T |\rho_i(t) - \bar{\rho}(t, y_i(t))|^2 dt. \quad (9)$$

The overall quality of the reconstruction is measured by the L^2 -norm of the error given by the Generalization Error (GE):

$$\text{GE}_T(\hat{\rho}) = \int_0^T \int_{y_1(t)}^{y_N(t)} |\rho(t, x) - \hat{\rho}(t, x)|^2 dx dt. \quad (10)$$

Problem statement: The objective of this paper is to propose an efficient and algorithmic approach to get a density reconstruction with a low GE using possibly noisy measurements from PVs.

To get a small GE, there are two options:

- 1) There are many probe vehicles and then $\text{GE}_T(\hat{\rho}) \simeq \frac{1}{N} \sum_{i=1}^N \int_0^T |\rho_i(t) - \hat{\rho}(t, y_i(t))|^2 dt$, so a density reconstruction will lead to a small error;
- 2) The set \mathcal{H}_c is defined in such a way that the only possible minimizers have low GE.

Of course, we assume that the penetration rate is low, meaning that there are few probe vehicles compared to the number of vehicles. Hence the generalization error in the first case will be high if $\mathcal{H}_c = H^1(\Omega, H^2(\mathbb{R}, \mathbb{R}))$.

In this paper we are interested in the second case. The set \mathcal{H}_c is constructed using the fact that the probe vehicles' trajectories and the density must obey (8). In other words, the set \mathcal{H}_c is defined as follows:

$$\mathcal{H}_c = \left\{ \bar{\rho} \in C^1(\Omega, C^2(\mathbb{R}, \mathbb{R})) \mid \int_0^T \int_{y_1}^{y_N} \mathcal{N}_\rho[\bar{\rho}, v]^2 = 0 \text{ for } v \in \underset{\bar{v} \in C^2([0, 1], \mathbb{R}_{\geq 0})}{\text{Argmin}} \sum_{i=1}^N \int_0^T |v_i(t) - \bar{v}(\rho_i(t))|^2 dt \text{ s. t. } \int_0^1 \max \left(0, \mathcal{N}_v[\bar{v}] \Big|_{\rho=u} \right)^2 du = 0 \right\}.$$

Remark 5: It has been proven in [3] that the three conditions of Definition (1) imply perfect reconstruction for a large but finite T . A consequence is that for any density reconstruction in \mathcal{H}_c we get:

$$\lim_{T \rightarrow \infty} \text{GE}_T(\hat{\rho}) = 0. \quad \square$$

The following section gives some explanation about the costs, their meaning and how to locally solve optimization problem (9).

IV. LEARNING-BASED DENSITY RECONSTRUCTION

There are several solutions when dealing with constrained optimization. One is to define the optimized variables in such a way that the constraints are already satisfied as done in [22] where the boundary conditions are enforced in the solution. However, this technique does not work well in the presence of noise or for complex systems. Indeed, enforcing the satisfaction of some constraints can lead to a highly suboptimal solution since the total cost might get stuck at a saddle point. We will explore here a second solution, which consists of using an extended Lagrangian cost function.

Remark 6: We assume here that the measurements over a period $[0, T]$ are given as a dataset of finite size. That means the measurements are not functions but N_{meas} values at the sampling instants $\{t_k\}_{k=1}^{N_{\text{meas}}}$. \square

The Lagrange multiplier method relaxes the optimization problem (9) to:

$$\hat{\rho} \in \underset{\bar{\rho} \in C^1(\Omega, C^2(\mathbb{R}, [0, 1]))}{\text{Argmin}} \left\{ \min_{v \in C^2([0, 1], \mathbb{R}_{\geq 0})} \sum_k \lambda_k \mathfrak{L}_k \right\} \quad (11)$$

for $\lambda_k \geq 0$ and where the costs \mathfrak{L}_k are given in the following subsections.

A. Interpretation of the different costs

1) *Data-based costs:* The first kind of cost comes from traditional machine learning for regression purposes [23]. They consist of Mean Square Errors (MSE) between the measurements and the estimated function. Since we assume that the position measurements might be noisy, there are three data-based costs.

- 1) We measure the position of each PV at given instants t_k so that the dataset is $\{y_i(t_k)\}_{i,k}$. The MSE is

$$\mathfrak{L}_1 = \frac{1}{N} \sum_{i=1}^N \frac{1}{N_{\text{meas}}} \sum_{k=1}^{N_{\text{meas}}} \{y_i(t_k) - \hat{y}_i(t_k)\}^2.$$

Here, $\hat{y}_i : [0, T] \rightarrow \mathbb{R}$ is the estimated position of PV i .

- 2) The second data-based cost is related to the density measurements $\{\rho_i(t_k)\}_{i,k}$. The MSE is then similar to the previous case:

$$\mathfrak{L}_2 = \frac{1}{N} \sum_{i=1}^N \frac{1}{N_{\text{meas}}} \sum_{k=1}^{N_{\text{meas}}} \{\rho_i(t_k) - \hat{\rho}(t_k, y_i(t_k))\}^2$$

where $\hat{\rho} : [0, T] \times \mathbb{R} \rightarrow [0, 1]$ is the estimated density.

- 3) Finally, the last cost is new compared to the study done in [12] and is related to velocity measurements. This enables the possibility of reconstructing the model (8) by estimating the velocity function such that:

$$\mathfrak{L}_3 = \frac{1}{N} \sum_{i=1}^N \frac{1}{N_{\text{meas}}} \sum_{k=1}^{N_{\text{meas}}} \{v_i(t_k) - \hat{v}(\rho_i(t_k))\}^2$$

where $\hat{v} : [0, 1] \rightarrow \mathbb{R}_{\geq 0}$ is the estimated velocity.

These costs are fully data-driven, meaning that they are based on data only, so they provide quantitative information which can be used to reject *unbiased* noise.

However, there are drawbacks. First, in the presence of biased noise, the previous cost functions do not perform well. Indeed, space and density measurements are used directly in the reconstructed density ($\hat{\rho}(t_k, y_i(t_k))$) and reconstructed speed ($\hat{v}(\rho_i(t_k))$). Secondly, we must have as many density measurements as position and speed measurements. One solution to these problems is to introduce two other costs:

- 1) The first one is to correct for error in the trajectory measurements:

$$\mathfrak{L}_4 = \frac{1}{N} \sum_{i=1}^N \frac{1}{N_{\text{meas}}} \sum_{k=1}^{N_{\text{meas}}} [\rho_i(t_k) - (\hat{\rho}(t_k, \hat{y}_i(t_k)) - n_{\rho_i})]^2$$

where n_{ρ_i} is a variable introduced to suppress the bias in the noise (as discussed in [12]).

- 2) The second cost is related to velocity measurements:

$$\mathfrak{L}_5 = \frac{1}{N} \sum_{i=1}^N \frac{1}{N_{\text{meas}}} \sum_{k=1}^{N_{\text{meas}}} [v_i(t_k) - \hat{v}(\hat{\rho}(t_k, \hat{y}_i(t_k)) - n_{\rho_i})]^2.$$

Remark 7: Note that we do not consider an extra variable to remove the biases on the trajectories since they are defined up to a constant. There is no correction for bias on the velocity measurements since these measurements are assumed not to be subject to noise. \square

Finally, the most important deficiency when using only data-based costs is the necessity of a large dataset. More specifically, the measurements should be well spread across the set $[0, T] \times [y_1, y_N]$. In our case, this is not true since the measurements are taken along the trajectories of the PVs.

To ensure a small generalization error, one then needs to introduce other kinds of cost functions.

2) *First order physics cost:* This cost is called a first order physics cost since it depends not only on measurements but also on the physics of the system by assuming some underlying dynamics.

$$\mathfrak{L}_6 = \frac{1}{N} \sum_{i=1}^N \frac{1}{N_{\text{meas}}} \sum_{k=1}^{N_{\text{meas}}} \left\{ \dot{\hat{y}}_i(t_k) - \hat{v}(\rho_i(t_k) - n_{\rho_i}) \right\}^2.$$

This is a mixed data/model driven cost and it is useful for identification. Indeed, this is an additional cost that uses the function \hat{v} , consequently, it can be used to enhance the identification by removing the bias from density measurements. It can be seen as a feedback on the speed function.

3) *Second order physics costs:* The second order costs do not depend on measurements but use the reconstructed functions only. Consequently they can be seen as regularizers.

- 1) Dynamics of the traffic density: given N_{phy}^{ρ} sample points $\{(t_k^{\rho}, x_k^{\rho})\}_{k=1}^{N_{\text{phy}}^{\rho}}$,

$$\mathfrak{L}_7 = \frac{1}{N_{\text{phy}}^{\rho}} \sum_{k=1}^{N_{\text{phy}}^{\rho}} \left(\mathcal{N}_{\rho}[\hat{\rho}, \hat{v}] \Big|_{(t,x)=(t_k^{\rho}, x_k^{\rho})} \right)^2$$

Simultaneously, the dissipation coefficient γ that is introduced to ensure convergence of the neural network

[8], [12] needs to be small, leading to the introduction of another cost:

$$\mathcal{L}_8 = \gamma^2.$$

- 2) Dynamics of the PVs' trajectories: given N_{phy}^y sample points $\{t_k^y\}_{k=1}^{N_{\text{phy}}^y}$,

$$\mathcal{L}_9 = \frac{1}{N} \sum_{i=1}^N \frac{1}{N_{\text{phy}}^y} \sum_{k=1}^{N_{\text{phy}}^y} \left(\mathcal{N}_y[\hat{y}_i] \Big|_{t=t_k^y} \right)^2$$

- 3) Constraint on the concavity of f : given N_{phy}^v sample points $\{\rho_k^v\}_{k=1}^{N_{\text{phy}}^v}$,

$$\mathcal{L}_{10} = \frac{1}{N_{\text{phy}}^v} \sum_{i=1}^{N_{\text{phy}}^v} \max \left(0, \mathcal{N}_v[\hat{v}] \Big|_{\rho=\rho_k^v} \right)^2$$

These three costs do not depend on the data at all but are rather based on the assumption that the real dynamics follow equation (8). The advantages are the same as in any model-based framework: they can effectively reduce the noise. However, in the context of state reconstruction, the initial condition is unknown (that can be given by the data-based costs). Consequently, they tend to force the convergence to the zero solution. In that sense, they are adversarial to the data-based costs since minimizing one type of cost often implies maximizing the other type.

4) *Total cost*: The total cost is then a weighted sum of the ten previously introduced loss functions pondered by $\{\lambda_k\}_k$. If $\lambda_2, \lambda_3, \lambda_7$ and λ_9 are all strictly positive, then the penalty method [24] states that solving a sequence of problems with these weight variables increasing and going to infinity leads to a solution to the discretized original problem (9).

The remaining cost functions are used to enhance the quality of the reconstruction by restraining the set of possible solutions and rejecting the noise. Indeed, the trajectory reconstructions suppress the possibly *unbiased* noise on the locations of the local density measurements. The costs related to the speed are used for identification. It appears in fact that using a subset of all the velocity measurements is enough since the identification is also supported by the cost functions $\mathcal{L}_5, \mathcal{L}_6, \mathcal{L}_7, \mathcal{L}_9$ and \mathcal{L}_{10} .

Note than in the original papers [7], [8], physics-informed optimization problems use only data-based and 2nd order physics costs. The 1st order physics cost is introduced here since it can help reducing the noise in the measurements (it is partly model-based) and helps for identification. However, it does not correct for sparsity in the measurements since it depends on the data-set.

B. Neural network approximation of a density reconstruction

Let Θ_θ be a general neural network of a given architecture where the parameters (such as weights and biases) are given by the tensor θ . We propose to approximate a function $\hat{\rho}$ satisfying (11) by Θ_θ .

It has been proved in [8] and [12, extended version] that a density reconstruction can be approximated as well as we desire by a neural network provided that there are enough

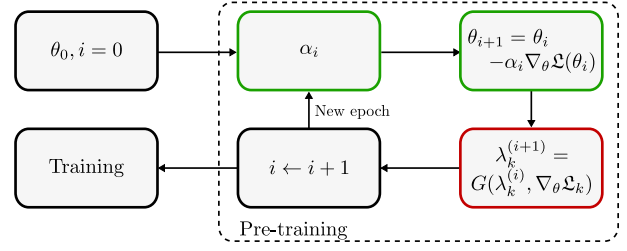


Fig. 1. Flow diagram of the update process. The boxes in green refer to traditional 1st order optimization scheme. The red box refers to the hyper-parameters λ_k update. The function G is defined such that (12) holds.

neurons. Consequently, for a large neural network, the main issue is then to solve (11).

1) *Training procedure*: The optimization problem (11) is particularly difficult to solve since it involves many ‘adversarial’ costs. In that scenario, standard optimization algorithms might not minimize the costs that are slowly varying with respect to the parameters tensor θ . To the best of the authors’ knowledge, the article [25] is the first to try to tackle this problem by adapting the weights $\{\lambda_k\}$ during the training. However, the algorithm is sensitive to noise and lacks intuition. Based on the same idea, we propose here a simplified version of a new adaptive algorithm.

The idea behind the algorithm described in [25] is very simple. If one uses a gradient-descent based optimization algorithm, the update formula at step i will be:

$$\theta_{i+1} = \theta_i - \alpha_i \sum_{k=1}^{10} \lambda_k^{(i)} \nabla_\theta \mathcal{L}_k(\theta_i)$$

where α_i is the learning rate. In the case of more complex optimizers such as ADAM [26], this learning rate is updated at each epoch. To successfully reduce all the cost functions, the gradients of each $\lambda_k \mathcal{L}_k$ should be approximately equal in absolute value. That implies the following ‘balance-rule’:

$$\lambda_1^{(i+1)} \overline{|\nabla_\theta \mathcal{L}_1|} = \dots = \lambda_{10}^{(i+1)} \overline{|\nabla_\theta \mathcal{L}_{10}|} = \frac{\sum_{k=1}^{10} \lambda_k^{(i)} \overline{|\nabla_\theta \mathcal{L}_k|}}{10}. \quad (12)$$

The operation $\bar{\cdot}$ corresponds to average since the gradients are usually vectors. The fact that all the weighted sum should remain the same is a novelty compared to [25] and helps to stabilize the update process.

The training procedure is summarized in Figure 1 and is divided into two parts:

- **Pre-training**: We use a 1st order algorithm (such as stochastic gradient descent, ADAM...) combined with the lambda updating process described earlier. To be less stochastic, the updates of the λ_i are done with memory and not at each epoch.
- **Training**: the pre-training helped in selecting weighting terms such that the loss is now equally balanced between each sub-loss functions. The second step aims at ensuring the convergence to the minimal value of the cost. The best is then to use a second-order optimizer such as BFGS.

2) *Network architecture*: As explained in [12], multilayer neural networks with tanh activation function provide an effective and simple architecture for this problem. There is not much difference for the density reconstruction: one multilayer neural network for the density which takes two inputs. Thanks to the previous training procedure, the convergence is very fast and it is quite robust with respect to the network initialization. Compared to [12], we do not require a very large neural network to ensure convergence to a good local optimum.

In this case, we considered 5 hidden layers with 10 neurons each. So that the standardized density remains in $[-1, 1]$, we propose the application of a last tanh function after the output of the neural network. The neural network architecture is slightly different for the probe vehicles trajectories. Here we use one small neural network per vehicle: 3 hidden layers with 5 neurons each.

A neural network to estimate the speed function v is also required. Since the function should not be too complex (otherwise it will be very difficult to solve the PDE), we propose a very simple multi-layer neural network, e.g. 1 input, two hidden layers with 5 neurons each and 1 output. We force $v(1) = 0$ by multiplying the network output by $1 - \hat{\rho}$.

V. SIMULATION RESULTS & DISCUSSION

In this section, we first compare some given simulation results and then investigate the performance of the training procedure using a statistical analysis¹.

A. SUMO simulation

A SUMO simulation was conducted and after convolution with an exponential kernel, one gets Figure 2a. One can clearly see stop and go waves which originate from a traffic light located at $x = 2.5$ km. Due to space restrictions, we show here only the result in the more complex case. Simulations using the Greenshield and Newell-Daganzo flux functions have also been conducted.

The reconstruction using the methodology of this paper gives the estimated density in Figure 2b. The characteristics are well-identified and the result is smoother than the original density. The generalization error is small (0.3) and this reconstruction can be used for control. The main advantage of this method is its ability to predict future values. This is however not discussed here.

To obtain such a result, we considered a relatively low number of physical points $N_{\text{phy}}^{\rho} = 500$. The reason behind this choice is very simple: SUMO uses a second order follow the leader and approximating it using a first order hyperbolic equation would lead to discrepancies. However, with a low N_{phy}^{ρ} , the model is enforced only when data is not available, thus ensuring a relatively good fit.

The scalability of the method to a large number of PVs is however to be investigated. The problem comes from the explosion of neurons (there is one small neural network per

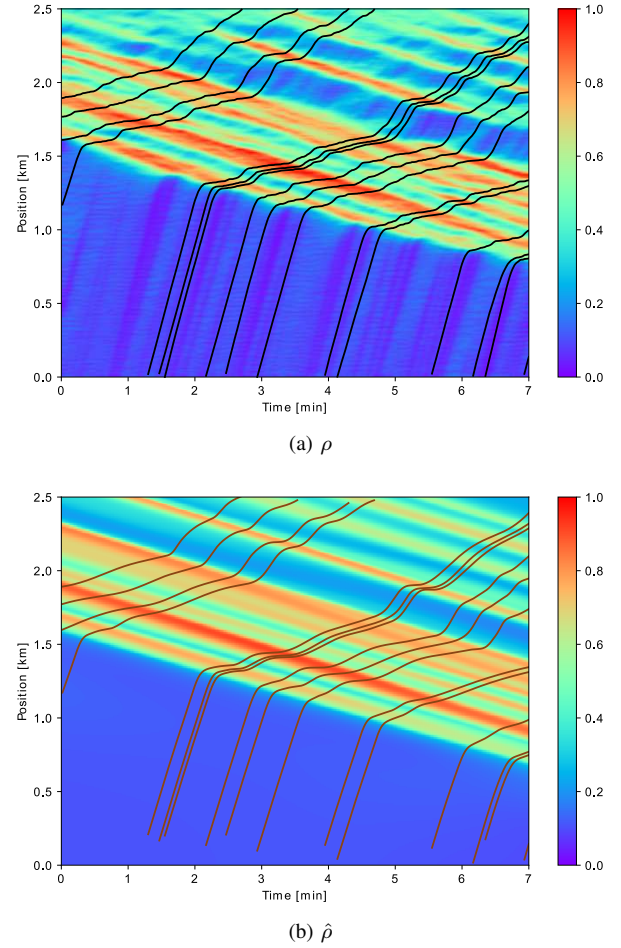


Fig. 2. Reconstruction for the SUMO simulation. (a) normalized density from a SUMO simulation, black lines represent the PVs' trajectories. (b) estimated reconstructed density using a neural-network, brown lines represent the estimated PV trajectories.

PV). Since the neural networks are not interconnected, the memory requirements are proportional to the number of PVs.

B. Training performances

We investigate here the computation time and error for three simulation cases:

- 1) density measurements computed using a Godunov solver for (1) with the Greenshields flux function (4);
- 2) density measurements computed using a Godunov solver for (1) with the flux function (5);
- 3) density measurements from the SUMO simulation.

The distribution of the computation time and mean square density error for 50 simulation runs of each case are shown in Figures 3 and 4, respectively. The simulations were run on a laptop with an Intel(R) Core(TM) i5-8365U CPU @ 1.60 GHz with four processor cores. The MSE is a discretized version of the generalization error introduced in (10) where the ground truth density is obtained either using the Godunov scheme or from SUMO, depending on the simulation case.

VI. CONCLUSION & PERSPECTIVES

In this article, we have investigated the use of physics-informed learning for identification and state reconstruction

¹The code is available on GitHub.

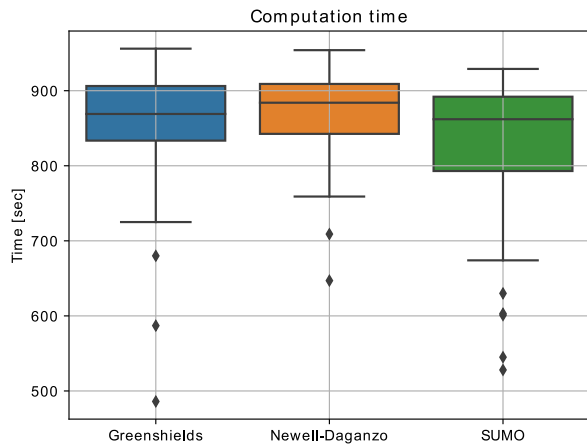


Fig. 3. Distribution of the computation time for each of the three simulation cases described in V-B, plotted from 50 simulation runs of each case.

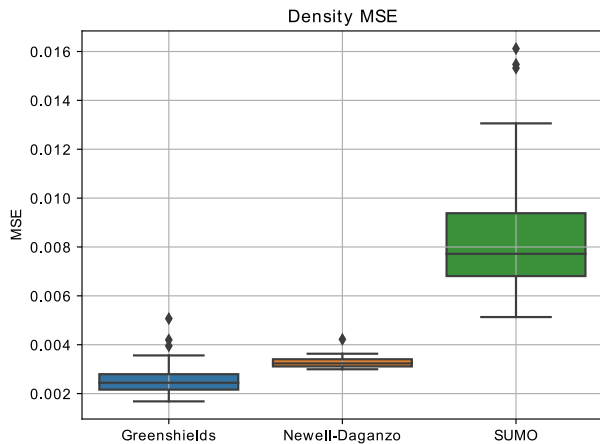


Fig. 4. Distribution of the density MSE for each of the three simulation cases described in V-B, plotted from 50 simulation runs of each case.

of traffic flow. The results show a good reconstruction quality with a moderate computational burden. The proposed training procedure helps in dealing with many physics costs and ensures a faster and more robust convergence.

However, there are some discrepancies in the reconstruction using data from SUMO. These might be due to the model used in this case. A second order scheme, including speed dynamics, seems to be a better choice and will be explored in a future paper. The extension to predictions in the near future should also be considered.

REFERENCES

- [1] A. Ferrara, S. Sacone, and S. Siri, *Freeway Traffic Modelling and Control*. Springer Nature, 2018.
- [2] T. Seo, A. M. Bayen, T. Kusakabe, and Y. Asakura, "Traffic state estimation on highway: A comprehensive survey," *Annual Reviews in Control*, vol. 43, pp. 128–151, 2017.
- [3] M. L. Delle Monache, T. Liard, B. Piccoli, R. Stern, and D. Work, "Traffic reconstruction using autonomous vehicles," *SIAM Journal on Applied Mathematics*, vol. 79, no. 5, pp. 1748–1767, 2019.
- [4] M. Barreau, A. Selivanov, and K. H. Johansson, "Dynamic traffic reconstruction using probe vehicles," in *Conference on Decision and Control (CDC)*, Jeju Island, Republic of Korea, 2020.
- [5] J. Berberich, A. Koch, C. W. Scherer, and F. Allgöwer, "Robust data-driven state-feedback design," in *2020 American Control Conference (ACC)*. IEEE, 2020, pp. 1532–1538.
- [6] J. C. Herrera and A. M. Bayen, "Incorporation of lagrangian measurements in freeway traffic state estimation," *Transportation Research Part B: Methodological*, vol. 44, no. 4, pp. 460–481, 2010.
- [7] M. Raissi, P. Perdikaris, and G. E. Karniadakis, "Physics-informed neural networks: A deep learning framework for solving forward and inverse problems involving nonlinear partial differential equations," *Journal of Computational Physics*, vol. 378, pp. 686–707, 2019.
- [8] J. Sirignano and K. Spiliopoulos, "DGM: A deep learning algorithm for solving partial differential equations," *Journal of computational physics*, vol. 375, pp. 1339–1364, 2018.
- [9] J. Huang and S. Agarwal, "Physics informed deep learning for traffic state estimation," in *2020 23rd International Conference on Intelligent Transportation Systems (ITSC)*. IEEE, 2020.
- [10] R. Shi, Z. Mo, K. Huang, X. Di, and Q. Du, "Physics-informed deep learning for traffic state estimation," *arXiv preprint arXiv:2101.06580*, 2021.
- [11] B. T. Thodi, Z. S. Khan, S. E. Jabari, and M. Menendez, "Incorporating kinematic wave theory into a deep learning method for high-resolution traffic speed estimation," *arXiv preprint arXiv:2102.02906*, 2021.
- [12] M. Barreau, J. Liu, and K. H. Johansson, "Learning-based state reconstruction for a scalar hyperbolic PDE under noisy lagrangian sensing," in *Learning for Dynamics and Control*. PMLR, 2021.
- [13] J. Liu, M. Barreau, M. Čičić, and K. H. Johansson, "Learning-based traffic state reconstruction using probe vehicles," in *16th IFAC Symposium on Control in Transportation Systems (CTS)*, 2021.
- [14] M. Behrisch, L. Bieker, J. Erdmann, and D. Krajzewicz, "SUMO – Simulation of Urban MObility; An Overview," *German Aerospace Centre, Institute for Transportation Research*, 2011.
- [15] M. J. Lighthill and G. B. Whitam, "On kinematic waves II. a theory of traffic flow on long crowded roads," *Proceedings of the Royal Society of London. Series A. Mathematical and Physical Sciences*, vol. 229, no. 1178, pp. 317–345, 1955.
- [16] C. M. Dafermos, *Hyperbolic Conservation Laws in Continuum Physics; 3rd ed.*, ser. Grundlehren der mathematischen Wissenschaften. Dordrecht: Springer, 2010.
- [17] B. D. Greenshields, J. R. Bibbins, W. S. Channing, and H. H. Miller, "A study of traffic capacity," in *Highway research board proceedings*, vol. 14. National Research Council (USA), Highway Research Board, 1935.
- [18] G. F. Newell, "A simplified theory of kinematic waves in highway traffic, part i: General theory," *Transportation Research Part B: Methodological*, vol. 27, no. 4, pp. 281–287, 1993.
- [19] C. F. Daganzo, "The cell transmission model: A dynamic representation of highway traffic consistent with the hydrodynamic theory," *Transportation Research Part B: Methodological*, vol. 28, no. 4, pp. 269–287, 1994.
- [20] R. M. Colombo and E. Rossi, "On the micro-macro limit in traffic flow," *Rendiconti del Seminario Matematico della Università di Padova*, vol. 131, 2014.
- [21] R. Chellappa, G. Qian, and Q. Zheng, "Vehicle detection and tracking using acoustic and video sensors," in *2004 IEEE International Conference on Acoustics, Speech, and Signal Processing*, vol. 3. IEEE, 2004, pp. iii–793.
- [22] I. E. Lagaris, A. Likas, and D. I. Fotiadis, "Artificial neural networks for solving ordinary and partial differential equations," *IEEE transactions on neural networks*, vol. 9, no. 5, pp. 987–1000, 1998.
- [23] I. Goodfellow, Y. Bengio, and A. Courville, *Deep Learning*. MIT Press, 2016.
- [24] D. P. Bertsekas, *Constrained optimization and Lagrange multiplier methods*. Academic press, 2014.
- [25] S. Wang, Y. Teng, and P. Perdikaris, "Understanding and mitigating gradient pathologies in physics-informed neural networks," *arXiv preprint arXiv:2001.04536*, 2020.
- [26] D. P. Kingma and J. Ba, "Adam: A method for stochastic optimization," in *3rd International Conference for Learning Representations*, 2015.